

# HIGHLY SENSITIVE COMPACT ISFET ELECTRO-CHEMICAL SENSOR IN AVALANCHE REGION OF OPERATION

Mohammad Mohiuddin Uzzal<sup>1</sup>

**Abstract-** In this paper we present an analytical model of sensitivity for ion sensitive field effect transistor (ISFET) in different region of operation, including Avalanche region. Electro-chemical based ISFET sensor performance is heavily dependent on DC bias and operational region of the sensor. Here, we present a comparative analysis of ISFET sensitivity while the operational region is changed. Using our developed model, we find an optimum bias point to ensure maximum sensitivity from a tiny nanoscale ISFET sensor. Based on SPICE simulations, it is shown that for a minimum size N-type ISFET (W/L=2) using TSMC's 0.25um fabrication process, we can achieve the sensitivity of about 14nA of current change per unit change of pH. However, we can derive higher sensitivity from the same device by operating the device in avalanche region of operation with high avalanche multiplication factor, M.

**Keywords –** Sensitivity, CMOS Compatibility, pH-to-current, ISFET, Avalanche region, Avalanche multiplication, Electro-Chemical sensor.

## 1. INTRODUCTION

Electro-chemical sensors based on the ion-sensitive field effect transistors (ISFET) was first proposed and fabricated by Bergveld [1]. ISFETs have been intensively investigated because of their compatibility with complementary metal-oxide-semiconductor (CMOS) manufacturing technologies, portability, miniaturized integrated transduction and the label-free detection of bio-molecule [2], [3], [4]. Generally, different ion-sensitive materials (Al<sub>2</sub>O<sub>3</sub>, Si<sub>3</sub>N<sub>4</sub>, Ta<sub>2</sub>O<sub>5</sub>, SnO<sub>2</sub>, SiO<sub>2</sub>) are used in gate of ISFET on the basis of their stability, sensitivity, selectivity, long-term drift, temperature dependency, responses time etc. The gate insulator of the ISFET senses the specific ion concentration, and generates an interface potential at the gate. This interface potential change at gate, causes drain-source current change in the semiconductor channel.

The sensitivity of an ISFET is proportional to  $\Delta I_{ds}/\Delta V_T$ , where  $\Delta I_{ds}$  is the change in the drain source current and  $\Delta V_T$  is change of interface potential at gate, due to the capture or adsorption of analytes. The more sensitive the sensor is, the more is the change in channel current for each unit change of interface potential. References [5], [6], [7], [8] and [9], recommend sub-threshold operation of ISFET to maximize sensitivity as drain current at sub-threshold regime increases exponentially with small gate perturbations. The drain current in ISFET at avalanche region of operation also increases exponentially, due to carrier multiplication effect. The avalanche process in FET occurs when the carriers in the channel are accelerated by the electric field of energies sufficient to free electron-hole pairs via collisions with bound electrons. The concept of avalanche sensing is widely used in image sensing i.e. imaging, spectroscopy, cryptography etc. [10], [11], [12], [13] due to their high sensitivity in avalanche region. The variation of drain-source current with change of operational region is shown in Fig. 1.

In this article, we present an analytical model of ISFET sensitivity while the region of operation changes. This paper is organized as follows: Section II discusses on ISFET sensor structure and biasing. In section III, an analytical model of ISFET sensitivity is developed. Simulation results are discussed and presented in section IV. Finally, the conclusions are drawn in Section V.

## 2. ISFET SENSOR STRUCTURE AND BIASING

The current through ISFET can be modeled with that of MOSFET. As stated by inventor, Bergveld [1], “The ISFET is in fact nothing else than a MOSFET with the gate connection separated from the chip in the form of a reference electrode inserted in an aqueous solution which is in contact with the gate oxide”. The threshold voltage of ISFET is given by [14]-

$$V_T = E_{ref} - \psi_0 + \chi_{solution} - \frac{\phi_{Si}}{q} - \frac{Q_{ox} + Q_{ss} + Q_B}{C_{ox}} + 2\phi_f \quad (1)$$

where,  $E_{ref}$  is the constant potential of reference electrode,  $\psi_0$  is the interface potential at solution/oxide interface,  $\chi_{solution}$  is the surface dipole potential of the solvent,  $\phi_{Si}$  is the work function of the silicon,  $Q_{ox}$ ,  $Q_{ss}$  and  $Q_B$  are the oxide charge, oxide

<sup>1</sup> Electrical and Electronic Engineering Department, American International University – Bangladesh (AIUB), Kuril, Dhaka, Bangladesh

interface charge and bulk charge respectively,  $2\phi_f$  is the potential for inversion of channel and  $C_{ox}$  is the oxide capacitance /unit area.

Equation (1) can be simplified as in [15] to be-

$$V_T = V_{th(MOS)} + V_{chem} \quad (2)$$

where,  $V_{chem} = \gamma + 2.303 \cdot \alpha \cdot U_T \cdot \Delta pH$ . Here,  $\gamma$  is a group of pH independent chemical potential,  $\alpha$  is a dimensionless sensitivity parameter and,  $U_T = kT/q$  is the thermal potential. In an ideal case, where the highest sensitive interface materials (Ta2O5) is used on the gate,  $\alpha$  is approximately equal to 1 and  $U_T$  at room temperature is about 26mV. Based on (2), for every unit of pH change, we can achieve about 59.8mV of change in threshold voltage when Ta2O5 is used as gate interface material [14]. Therefore, as the pH of gate liquid increase, threshold voltage of ISFET increases too. This increment of threshold voltage causes reduced drain-source current  $I_{ds}$  of ISFET for a given bias condition, shown in Fig.2.

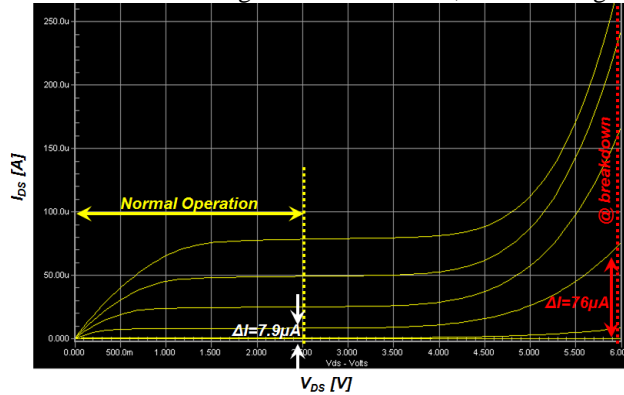


Fig.1: Variation of Drain-Source current with change of operational region.

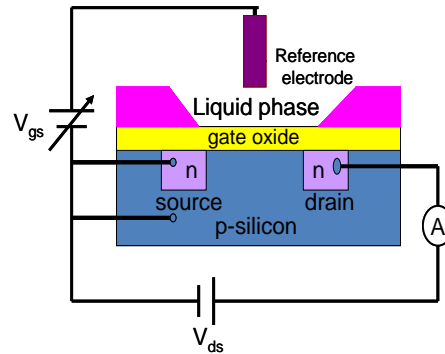


Fig.2: ISFET structure, bias and response.

### 3. ANALYTICAL MODEL OF ISFET SENSOR'S BIAS DEPENDENT SENSITIVITY

The sensitivity of an ISFET can be defined as the change of ISFET current due to the change of gate liquid pH i.e. ISFET ability to detect pH change. This pH sensitivity of ISFET is related with the change of ISFET current through the following relation.

$$S_{ISFET} = \frac{\Delta I_{DS}}{\Delta pH} = \frac{\Delta I_{DS}}{\Delta V_{GS}} \times \frac{\Delta V_T}{\Delta pH} = g_m \times \frac{\Delta V_T}{\Delta pH} \quad (3)$$

where  $S_{ISFET}$  is the sensitivity of our proposed ISFET device.

If we use Ta2O5 as interface material in ISFET gate, we can achieve a threshold voltage change of around for every unit of pH change [14]. Therefore, the sensitivity variation of ideal ISFET with pH change will become as shown in Fig. 4. We can achieve a sensitivity of around 30nA/pH for this ideal ISFET with  $W/L=2$ ,  $V_T=0.35$  V and  $K'n=150\mu A/V^2$ .

#### 3.1 Sensitivity of Long Channel Ideal ISFET

The current through drain to source of ISFET can be modeled with that of MOSFET. This drain to source current strongly depends on the  $V_{gs}$  and  $V_{ds}$  bias voltage sources of ISFET. Based on the magnitude of bias voltages of ISFET, we can differentiate the operating region of ISFET in three regions, which are i) Cut-off region ii) Linear region and iii) Saturation region. An ISFET operates in cutoff region when  $V_{gs} < V_T$ . At cutoff region of operation, both the current and sensitivity of ISFET is Zero.

Linear operating region of ISFET is dictated by the bias condition as below -  $V_{ds} < V_{gs} - V_T$  and  $V_{gs} > V_T$ . At linear operating region, the current and sensitivity of ISFET can then be modeled as:

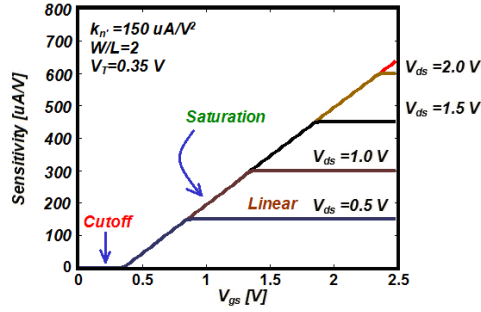


Fig. 3: Voltage-to-current sensitivity of an ideal ISFET.

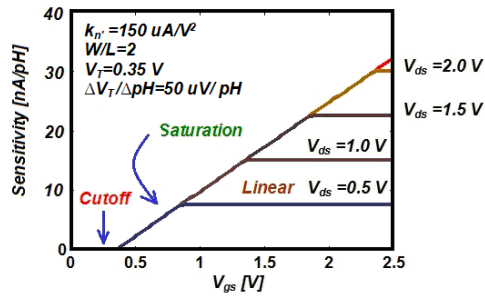


Fig. 4: pH to Current Sensitivity of an Ideal ISFET.

$$I_{ds} = \mu_n C_{ox} \frac{W}{L} \left[ (V_{gs} - V_T) V_{ds} - \frac{1}{2} V_{ds}^2 \right] \tag{4}$$

and  $\left| \frac{dI_{ds}}{dV_{gs}} \right| = \left| \frac{dI_{ds}}{dV_T} \right| = \mu_n C_{ox} \frac{W}{L} V_{ds}$  (5)

Where  $\mu_n$  is the mobility of electron,  $C_{ox}$  is the capacitance per unit area of the gate insulator,  $V_{ds}$  is drain to source bias voltage of ISFET,  $W$  is the channel width and  $L$  is the channel length of ISFET.

Based on (5), the sensitivity of ISFET at linear region is a linear function of the voltage of  $V_{ds}$  but it is independent of  $V_{gs}$  and  $V_T$  voltages.

However, the current and sensitivity of ISFET at saturation region, dictated by bias conditions,  $V_{ds} \Rightarrow V_{gs} - V_T$  and  $V_{gs} > V_T$ , can be modeled by:

$$I_{ds} = \mu_n C_{ox} \frac{W}{2L} [(V_{gs} - V_T)]^2 \tag{6}$$

and  $\left| \frac{dI_{ds}}{dV_{gs}} \right| = \left| \frac{dI_{ds}}{dV_T} \right| = \mu_n C_{ox} \frac{W}{L} (V_{gs} - V_T)$  (7)

Equation (7) shows that at saturation region ISFET sensitivity is independent of the voltage of  $V_{ds}$  but it is linearly dependent on  $V_{gs}$  and  $V_T$  voltages. We can also see that the effect of threshold voltage change on ISFET sensitivity is same as of  $V_{gs}$  voltage change, from (7).

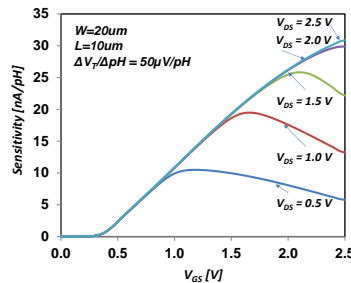


Fig. 5: Sensitivity of a Long Channel ISFET with  $W/L=2$ .

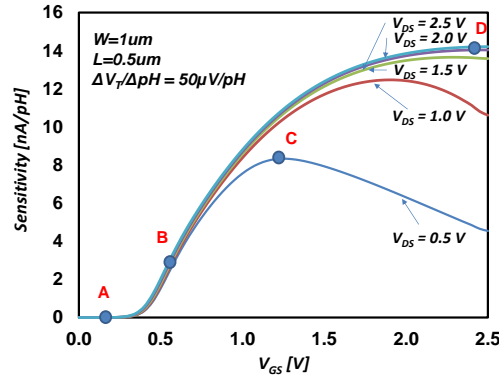


Fig. 6: Sensitivity of a short channel ISFET with  $W/L=2$ .

Fig. 3, shows the variation of ISFET sensitivity ( $\mu\text{A}/\text{V}$ ) when the voltage of  $V_{gs}$  is varied. The ISFET model, used in Fig. 3 did not consider the non-ideal effects. This ideal behavioral simulation of ISFET shows that for a given technology and device dimension, the maximum sensitivity is at saturation region when both  $V_{ds}$  and  $V_{gs}$  voltages are at their allowable maximum value. The actual sensitivity of ISFET is its ability to sense the change of pH. The interface material of  $\text{Ta}_2\text{O}_5$ , if used in ISFET gate gives us a threshold voltage change of around  $50\mu\text{V}$  for every unit of pH change [14]. Therefore, the sensitivity ( $\text{nA}/\text{pH}$ ) variation of ISFET with pH change will become as shown in Fig. 4. We can achieve a sensitivity of around  $30\text{nA}/\text{pH}$  for this ideal ISFET with  $W/L=2$ ,  $V_T=0.35\text{ V}$  and  $kn'=150\mu\text{A}/\text{V}^2$ . But, the actual sensitivity from a real non-ideal ISFET is of much lower value as shown in Fig. 5 and Fig. 6.

### 3.2 Sensitivity of Short Channel ISFET-

The SPICE simulation results for a long-channel N-type ISFET using TSMC's  $0.25\mu\text{m}$  technology model is shown in Fig. 5, when  $L=10\mu\text{m}$  and  $W/L=2$ . Note that due to mobility degradation of short channel ISFET, the sensitivity doesn't stay constant for a constant  $V_{DS}$ , as we predicted in Fig. 4. The short channel effects become more prominent when we reduce the channel length to  $L=0.5\mu\text{m}$  as shown in Fig. 6. Because of many issues in the short channel device, including, channel length modulation, velocity saturation, and drain induced barrier lowering (DIBL), the sensitivity of ISFET degrades when we shrink the device length. The maximum sensitivity of ISFET reduces from  $30\text{nA}/\Delta\text{pH}$  to about  $14\text{nA}/\Delta\text{pH}$  when the channel length reduces from  $10\mu\text{m}$  to  $0.5\mu\text{m}$  as shown in Fig. 5 and Fig. 6. We will discuss pros and cons of bias points A, B, C and D of Fig. 6, below.

**Bias point A:** At this bias point, ISFET operates in cut-off/sub-threshold region of operation. The sensitivity from ISFET in this point is quite low. But the power consumption at this point is also very low. Therefore, this point is suitable for ultra-low power applications where higher sensitivity is not an issue.

**Bias point B:** Here, ISFET operates in saturation region of operation and the non-idealities due to short channel effects did not take into effect. The sensitivity of ISFET around this region is a linear function of  $V_{GS}$  and hence sensitivity increases around bias point B as  $V_{GS}$  increases. However, the sensitivity of about  $4\text{nA}/\Delta\text{pH}$  may not be sufficient for many applications.

**Bias point C:** This point shows a local maximum of ISFET sensitivity. Beyond this bias point, the sensitivity degrades due to mobility degradation of carrier from short channel effects. We can bias ISFET to this sensitivity by applying  $V_{DS} = 0.5\text{ V}$  and  $V_{GS} = 1.25\text{ V}$ . The pH-to-current sensitivity at point C is near  $10\text{nA}/\text{pH}$ . This bias point gives us both high sensitivity and low power operation.

**Bias point D:** As we keep increasing of the voltage of  $V_{GS}$  and voltage of  $V_{DS}$ , ISFET enters into the region where short channel effects i.e. Mobility degradation, DIBL etc becomes so significant that the sensitivity of ISFET becomes saturated or degrades. For the given TSMC's  $0.25\mu\text{m}$  technology node - this bias point gives us maximum sensitivity from ISFET sensor at a price of high power consumption.

Therefore, for low power operation with high sensitivity, we should operate ISFET sensor at point C with optimum voltage of  $V_{GS}$  and  $V_{DS}$ . But for application that requires higher sensitivity we have to operate ISFET at bias point D where both  $V_{DS}$  and  $V_{GS}$  are close to maximum for a given technology node.

### 3.3 Sensitivity of ISFET in Avalanche Region -

For a n-MOS transistor that operate in saturation mode, if the generated current due to electron in channel is  $I_{DSat}$  and we assume the ionization rates for electron and hole are equal – then current in avalanche mode can be given as [16] by –

$$I_{DS} = MI_{DSat}$$

$$I_{sub} = (M - 1)I_{DSat}$$

and hence the sensitivity during avalanche mode is-

$$\frac{dI_{ds}}{dV_{th}} = \frac{\mu_n C_{ox} W}{M L} (V_{gs} - V_{th})^{-1} \tag{9}$$

which is M times higher than the sensitivity in saturation region. Where M, avalanche multiplication factor is defined as [16]

$$M = \left(1 - \int_0^{ld} \alpha dy\right)^{-1} \tag{10}$$

where ld is the width of the high field region where the avalanche multiplication occurs and is approximated by the empirical equation given by [17] –

$$ld = 0.22 t_{ox}^{1/3} x_j^{1/2} \tag{11}$$

And  $\alpha$  is the impact ionization rate and can be approximated by [18]  $\alpha = A \exp(-B/E)$  where E is the electric field, A and B are the ionization constants. Typical carrier flow in a MOSFET in avalanche mode of operation is shown in Fig. 7.

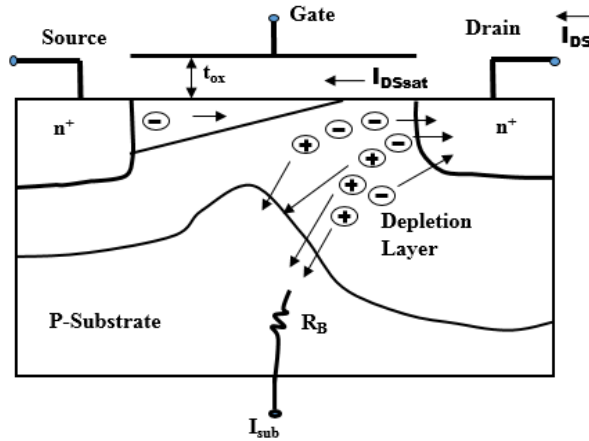


Fig. 7. Typical Current flow in a MOSFET during avalanche [16].

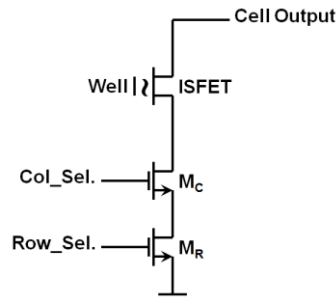


Fig. 8: Unit cell structure of the ISFET sensor.

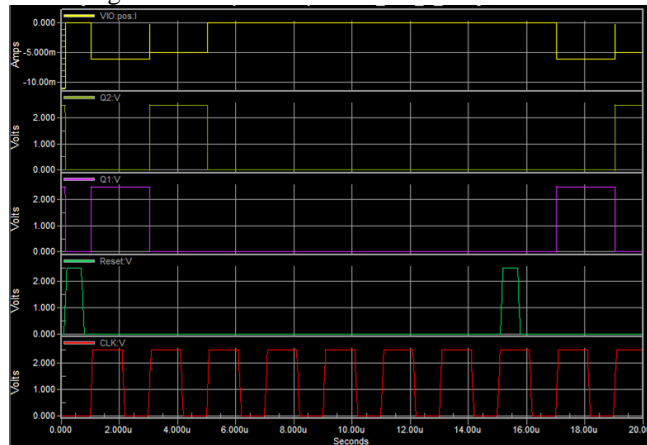


Fig. 9: SPICE simulation of ISFET sensor Unit Cell with clock, reset, column select pulses.

#### 4. UNIT CELL STRUCTURE AND SIMULATION RESULTS

Our objective in this research is to design a highly sensitive compact chip that have millions of ISFET sensor. In order able to access the sensing data from ISFET, each unit cell has two access transistors for row and column selections. The access transistors are designed large to make sure that it doesn't affect our ISFET measurements result. The structure of each unit cell with supporting access transistor is shown in the Fig. 8.

To confirm the functionality of the sensor with row and column select circuits, a SPICE simulation is performed on a smaller set of unit cell arrays. This simulation confirms the functionality of the row and column select circuits as well as ISFET sensor. We can see from Fig. 9 that after the reset and after each clock pulse, a column is selected where its output current is transferred to the output for further processing. It also confirms the functionality of ISFET sensor in operation.

#### 5. CONCLUSION

In this paper we had presented the concept of avalanche operation in electro-chemical based ISFET bio-sensor. We also presented an analytical model for ISFET sensor sensitivity in different region of operation, with a goal to ensure maximum sensitivity. We had also presented the proposed compact sensor structure with control circuitry for the ISFET sensor. To confirm the functionality of the unit sensor cell, we also performed SPICE simulation. The SPICE simulation result in transient domain confirms the perfect operation of the proposed compact ISFET sensor in operation.

#### 6. REFERENCES

- [1] P. Bergveld, "Development of an Ion-Sensitive Solid-State Device for Neurophysiological Measurements", IEEE Transactions on Bio-Medical Engineering, January 1970.
- [2] Chang-Soo Lee, Sang Kyu Kim and Moonil Kim, "Ion-Sensitive Field-Effect Transistor for Biological Sensing", Sensors 2009, 9, ISSN 1424-8220.
- [3] F. Uslu et al., "Label-free fully electronic nucleic acid detection system based on a field-effect transistor device" Biosensors and Bioelectronics -19 (2004).
- [4] Massimo Barbaro et al., "A CMOS, Fully Integrated Sensor for Electronic Detection of DNA Hybridization", IEEE Electron Device Letters, Vol. 27, No. 7, July 2006.
- [5] K. Shoorideh and Chi-On Chui, "Optimization of the Sensitivity of FET-Based Biosensors via Biasing and Surface Charge Engineering", IEEE Trans. on Electron Devices, Vol. 59, No. 11, Nov. 2012.
- [6] R.A. Chapman et al., "Comparison of Methods to Bias Fully Depleted SOI-Based MOSFET Nanoribbon pH Sensors", IEEE Trans. on Electron Devices, Vol. 58, No. 6, June 2011.
- [7] X.P.A. Gao et al., "Subthreshold Regime has the Optimal Sensitivity for Nanowire FET Biosensors", Nano Letter 2010, Feb. 10; NIH Public Access.
- [8] J. Ahn et al., "Nanowire FET Biosensors on a Bulk Silicon Substrate", IEEE Tran. on Electron Devices, Vol. 59, No. 8, Aug. 2012.
- [9] J. Ahn et al., "Double-Gate Nanowire Field Effect Transistor for a Biosensor", Nano Letter, Year 2010.
- [10] T. Watabe et al., "New Signal Readout Method for Ultrahigh-Sensitivity CMOS Image Sensor", IEEE Tran. on Elec. Devices, Vol. 50, No. 01, Jan. 2003.
- [11] G.F. Marshall et al., "Avalanche Photodiode-Based Active Pixel Imager", IEEE Tran. on Elec. Devices, Vol. 51, No. 03, Mar. 2004.
- [12] Chao Shi et al., "A Novel Asynchronous Pixel for an Energy Harvesting CMOS Image Sensor", IEEE Tran. On VLSI Systems, Vol. 19, No. 1, Jan. 2011.
- [13] Z. Xiao1 et al., "A New Single Photon Avalanche Diode in CMOS High-Voltage Technology", The 14th Int. Conf. on Solid-State Sensors, Actuators and Microsystems, Jun. 2007.
- [14] P. Bergveld, "Thirty years of ISFETOLOGY What happened in the past 30 years and what may happen in the next 30 years", Sensors and Actuators B, 2003.
- [15] L. M. Shepherd et al., "A Biochemical Trans-linear Principle With Weak Inversion ISFET's", IEEE Tran. On Circuits and Systems -I, Vol. 52, No. 12, Dec. 2005.
- [16] H. Wong, "A Physically Based MOS Transistor Avalanche Breakdown Model", IEEE Tran. On Electron Devices, Vol. 42, No. 12, Dec. 1995.
- [17] T.Y. Chan et al., "Dependence of Channel Electric Field on Device Scaling", IEEE Elec. Dev. Letters, Vol.6, No.10, Oct. 1985.
- [18] A.G. Chynoweth, "Ionization Rates for Electrons and Holes in Silicon", Physical Review, Vol. 109, No. 5, Mar. 1958.